A SOURCE MECHANISM FOR THE 7 APRIL 1958 HUSLIA, ALASKA EARTHQUAKE

Laura Reiser
Department of Geology
Beloit College
Beloit, WI 53511

INTRODUCTION

On April 7, 1958, at 15:30:40 (UT) a magnitude 7.3 earthquake shook Huslia, Alaska. Extensive sand flows, surface collapses, and ice cracking occurred in an area of approximately 400 square miles. The event was followed by four aftershocks with magnitudes above 6.0 over the next five weeks.

Despite its large magnitude, little work has been done on the main shock. This study is the first attempt at using modern techniques to determine the depth, fault geometry, and source time function of the earthquake.

DATA ACQUISITION AND PROCESSING

Because the Huslia earthquake occurred prior to the establishment of the World Wide Standardized Seismograph Network (WWSSN), the data set for the Huslia earthquake required requesting records from individual observatories. These records began trickling in to Trinity in October. By mid-January records from nine observatories had been received.

Since these seismograms were made prior to the standardization of instruments, each seismograph had unique characteristics. These must be known in order to include the instrument's response when creating a synthetic seismogram. Not all records were received with instrument characteristics. In addition, observatories were experimenting with their instrument responses; some of the seismographs were too sensitive, recording the earthquake off-scale. Also, many records have been destroyed or preserved in a useless fashion. For example, a Belgian observatory responded to our request for seismograms by saying they had transferred all records to 16mm film, thereby rendering them unusable for scientific study.

After receiving the seismograms and determining the instrument responses, the traces had to be digitized into the computer. This required tracing the peaks and troughs of the records using a digitizing table at Trinity.

Originally this study was to encompass the four aftershocks of the Huslia earthquake. However, few observatories sent both aftershock and main event records. The records of the aftershocks which were received appeared to be too small to be of value.

GEOLOGIC SETTING

Located at 65.75°N 155.75°W (Davis, 1960), the Huslia earthquake represents a rare event in the Koyukuk Basin south of the Brooks Range and north of the Ruby Geanticline (fig. 1). While there is a thrust fault in the Brooks Range and a strike slip fault in the Ruby Geanticline, there are no known fault traces near the focus of the Huslia earthquake. Using the fault geometry of the Huslia event in conjunction with other studies may provide a clue as to the stress field between the two known faults.

The Basin is composed of a volcanic arc assemblage consisting of Middle Jurassic to Early Cretaceous igneous rock (Patton and Box, 1989). The terrain near Huslia consists of sand dunes covering alluvial deposits from the meandering Koyukuk River (Davis, 1960).

FIRST MOTION ANALYSIS

Ritsema (1962) used the polarity of the first P wave arrivals to determine the strike and dip of one of the nodal planes as N 58°E, 64°SE. He could not completely constrain the second nodal plane using the first arrivals, but concluded that it must lie between N 8°W, 50°W and N 70°W, 38°NE. Because the damage zone trends N 70°E (Davis, 1960), Ritsema concluded that the fault plane must have a strike of N 70°E. Furthermore, because the second nodal plane must be perpendicular to the first, a fault with a strike of N 70°E must have a dip of 26°NW.

However, Ritsema used a crustal P velocity of 7.72 km/s. Analysis of data from earthquakes north of Fairbanks indicate a crustal P wave velocity of 6.1 km/s (Cady, 1989). A new focal mechanism was created using this new velocity with Ritsema's polarity determinations (fig. 2). This plot suggests a strike and dip of N 54°E, 70°SE for one of the nodal planes and a range between N 46°W, 64°NE and N 26°W, 63°SW for the other nodal plane. Furthermore, the trend of the damage zone does not define a second nodal plane along N 70°E. Body wave analysis indicates this is primarily a thrust fault. Therefore both nodal planes will have approximately the same strike. One nodal plane is constrained along N 54°E, which is close to the N 70°E suggested by the damage zone.

Table I: Synthetic P-wave parameters for the June 13, June 14, and June 22, 1975 aftershocks.

Aftershock:	**June 13, 1975**	**June 14, 1975**	**June 22, 1975**
Fault Plane:	N35E, 10NW	N35E, 5NW	N35E, 10NW
Slip Angle (°):	90.0	90.0	90.0
Depth (km):	6.0	8.0	8.0
Source Time Function:			
Rise time (sec):	2.0	2.0	3.0
Flat Time (sec):	10.0	10.0	7.0
Fall Time (sec):	2.0	2.0	2.0
Total (sec):	14.0	14.0	12.0

DISCUSSION:

Seismic moment is a product of the fault area, fault slip, and rigidity of the surrounding material (Stein et al., 1980). For earthquakes smaller than magnitude (M_S) 7.5, the seismic moment has an approximately linear relationship to the surface wave magnitude. Thus, by knowing the earthquake's magnitude, we can estimate the relationship between the rigidity and the movement along the fault plane. For example, if the rigidity is low, then the amount of slip would be relatively large. In this subduction zone setting, the rigidity is strongly controlled by depth.

Our analyses of the aftershocks reveals shallow depths, ranging from 6.0 - 8.0 km or 1-3 km under the ocean floor. This indicates placement of the foci of the aftershocks in the accretionary wedge as opposed to the more rigid oceanic crust. From the depths of the aftershocks, we infer that the mainshock also occurred at similar depths in the accretionary wedge. Our depths combined with the long source time function of the mainshock from previous studies suggest a large displacement which accounts for the ability of the shock to produce a large tsunami relative to its seismic moment.

REFERENCES CITED:

Asano, S., P. Yamada, K. Suyehiro, P. Yoshii, Y. Misawa, and S. Iizuka. 1980. Crustal structure in a profile off the Pacific Coast of Northeastern Japan by the refraction method with ocean bottom seismometers. *Journal of P-hysics of the Earth.* 29: 267-281.

Fukao, Y. 1979. Tsunami earthquakes and subduction processes near deep-sea trenches. *Journal of Geophysical Research.* 84: 2303-2314.

Kroeger, G. C., K. Shimazaki, and R. J. Geller. 1987. Source process of the June 10, 1975 Nemuro-Oki tsunami earthquake. *Eos Transactions.* 68: 1352.

Stein, S. and G. C. Kroeger. 1980. Estimating earthquake source parameters from seismological data. *Solid Earth Geophysics and Geotechnology*, edited by S. Nemat-Nasser, American Society of Mechanical Engineers, NY.

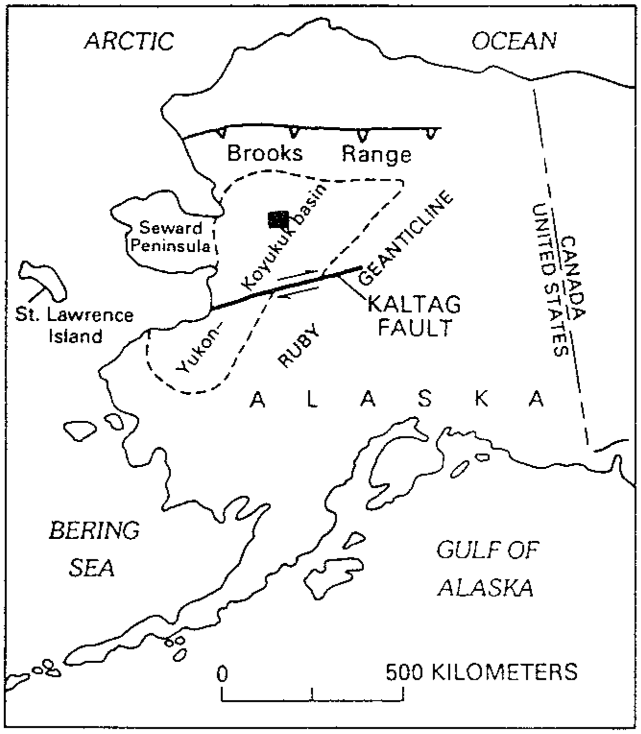

Figure 1. The Huslia earthquake was located at about 65.75°N 155.75°W as indicated by the solid square. The Koyukuk Basin is surrounded by a strike-slip fault to the south and a thrust fault to the north (modified from Patton and Box, 1989).

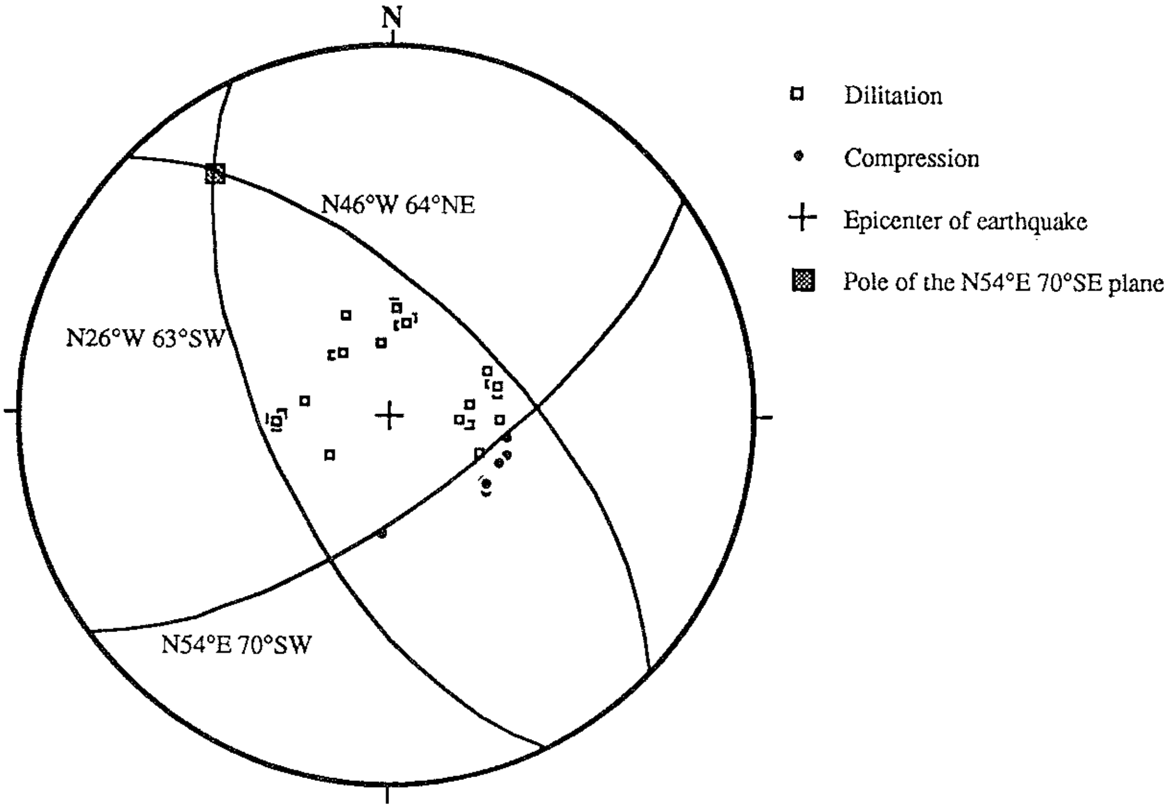

Figure 2. A focal mechanism created using P wave polarities from Ritsema (1962) with a P velocity of 6.1 km/sec. The nodal plane at N54°E 70°SW is well constrained. The other nodal plane must be perpendicular to the first nodal plane, passing through the pole indicated. The lines striking northwest show the limits of the values of this second plane.

Ritsema also used the S wave arrivals to assert that the Huslia earthquake had a single couple mechanism. Today seismologists believe that most earthquakes have a double couple mechanism. (Those with single couples are primarily caused by landslides or volcanic events.) The double couple and single couple mechanisms have the same P wave radiation patterns, but different S wave radiation patterns. Only in a single couple S wave radiation pattern can the fault plane can be distinguished from the auxiliary plane. The double couple mechanism became the accepted theory when WWSSN stations began providing overwhelming evidence in its favor.

BODY WAVE MODELLING

Using a body wave modelling program developed by Dr. Kroeger for the Macintosh II computer, a range of best fits for the depth, fault geometry, and source time function for the Huslia earthquake were determined (fig. 3). These ranges were found using the nodal plane along N 54°E, 70°SE determined by first motion techniques, and a structure profile of a 35 km thick crust with P wave velocity of 6.1 km/s overlying a 7.9 km/s upper mantle (Cady, 1989):

Depth: 5-7 km
Slip Angle: -90° ± 40°
Source Time Function: total length of 7 seconds ± 0.5
Rise Time: 2 seconds ± 0.5
Flat Time: 3 seconds ±1.0
Fall Time: 2 seconds ± 1.0

A slip angle of -90° corresponds to a thrust fault. The uncertainty of ± 40° is not uncommon for thrust faults, since the second nodal plane would only be constrained by using stations at the edges of the focal sphere. Good records at such stations are rare. Because the uncertainty is symmetric around 90° indicates there is very little strike slip movement.

These results fit well for the P waves, but not for the SH waves. The SH wave traces have an interesting common feature in the European records: the second trough is much greater in amplitude than the first trough (fig. 4). When a second source time function is introduced to add energy at the second trough in the SH waves, the P wave synthetics no longer match. Increases in depth cause the SH wave synthetics to lengthen, matching the overall form of the real records better. However, increased depth does not sufficiently increase the amplitude of the second trough. Furthermore, the increased depth disrupts the P wave match. If the first peak and trough of the SH wave trace are ignored, the 5-7 km depth fits reasonably well. However, there is no evidence indicating that this assumption is valid.

CONCLUSIONS

The Huslia earthquake of 7 April 1958 was along a thrust fault. The nodal plane determined by Ritsema (1962) has been modified slightly to N 54°E 70°SE. Furthermore, the earthquake had a double couple and not a single couple mechanism as he had concluded. Using body wave modelling techniques with P wave records a shallow depth of about 6 km and a source time function of 7 seconds have been determined. In the future the ranges for the nodal planes, depth, slip angle, and source time function may be constrained further with a better understanding of the SH wave records and by obtaining more seismograms of the event.

REFERENCES

Cady, John W., 1989, Geophysics of the Yukon-Koyukuk Province: Journal of Geophysical Research, v. 94, no. B11, p. 15821-15841.

Davis, Neil T., 1960, A field report on the Alaska earthquakes of April 7, 1958: Bulletin of the Seismological Society of America, v. 50, no. 4, p. 489-510.

Patton, William W., Jr., and Box, Stephen E., 1989, Tectonic setting of Yukon-Koyukuk Basin, Alaska: Journal of Geophysical Research, v. 94, no. B11, p. 15805-15820.

Ritsema, A. R., 1962, P and S amplitudes of two earthquakes of the single force couple type: Bulletin of the Seismological Society of America, v. 52, no. 4, p. 723-746.

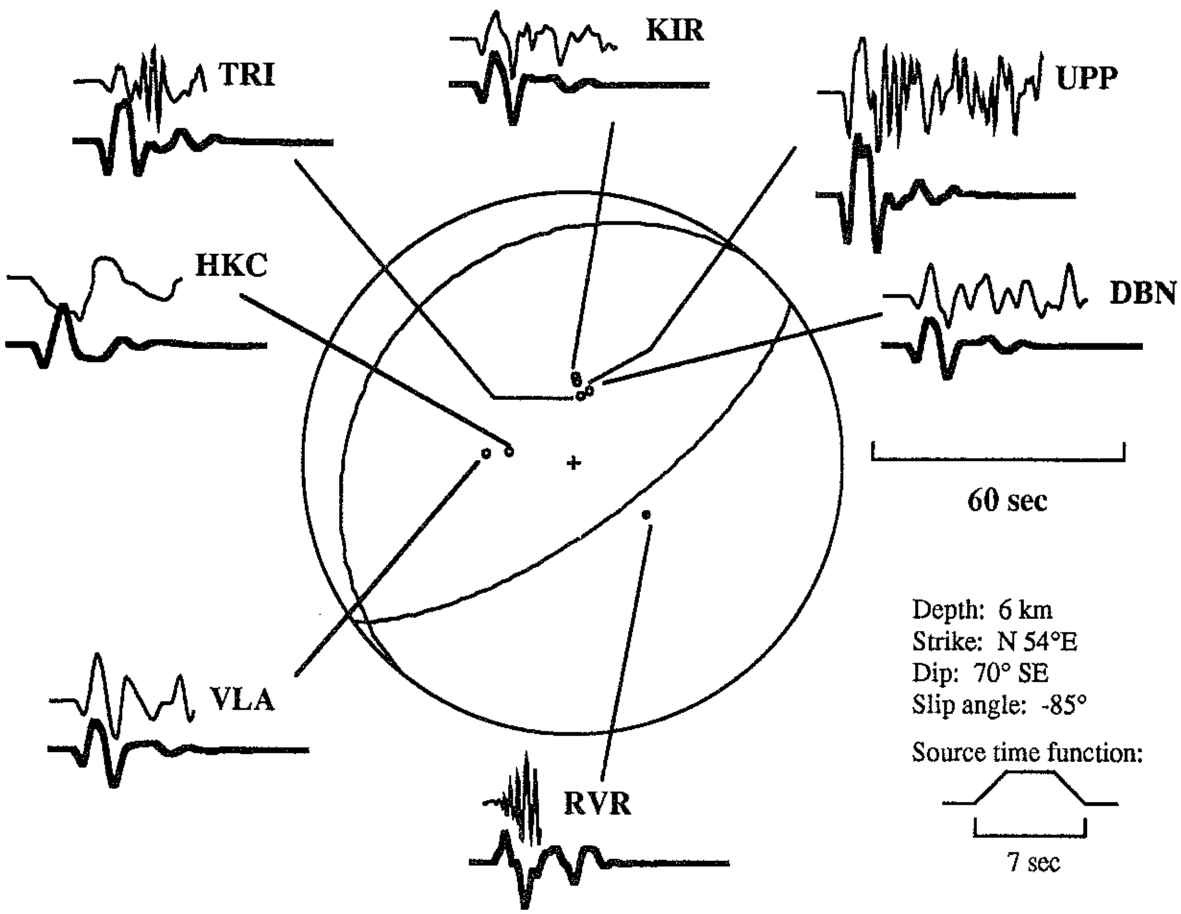

Figure 3. Observed P waves (top line) compared with synthetics (bottom line, bold). Although station HKC appears strange, the overall fit to the synthetics is good given the poor quality of the record. Because the instrument constant for station RVR is unknown, it is primarily valuable for polarity.

DBN is De Bilt, Netherlands
UPP is Uppsala, Sweden
KIR is Kiruna, Sweden
TRI is Trieste, Italy
VLA is Vladivostok, U.S.S.R.
HKC is Hong Kong
RVR is Riverside, California

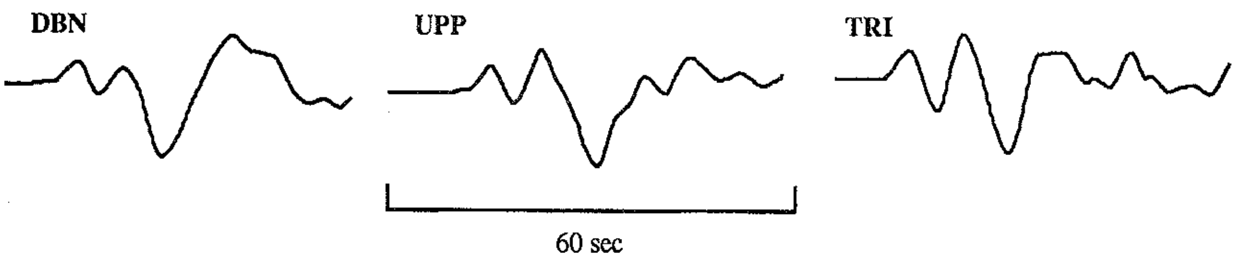

Figure 4. The SH wave forms from the European stations look strikingly similar. However, the depth which creates best fits for the P waves does not produce the second large trough observed in the above records.

FOCAL MECHANISM OF THE 30 JUNE 1975 YELLOWSTONE EARTHQUAKE FROM TELESEISMIC SH WAVE ANALYSIS

Greg Wimpey
Department of Geology
Trinity University
San Antonio, Texas 78212

Introduction

The June 30, 1975 Yellowstone earthquake had a local magnitude M_L=6.1. This is near the lower limit of the size of earthquake that can be easily studied using teleseismic body waves. For this reason, this is one of the few events in the western United States that has not be carefully studied. The difficulty in studying this event is compounded by a poor distribution of seismic stations in the distance range between 30° and 90° that is appropriate for teleseismic body wave modeling. Although there is reasonably good coverage to the north and east, the southwest coverage is missing because these distances fall in the Pacific ocean.

Robert Andrews has studied the P waves of this event. The results of that study, as well as an overview of the tectonics of the region are presented in the previous paper in this volume. The results of that study indicated a normal faulting mechanism with a focal depth of between 2.5 and 4.0 km (Andrews, personal communication). In addition, he found that a crustal model containing a low velocity zone improved the quality of the synthetic P wave fits. The P wave analysis was unable to provide adequate constraint on the strike or slip angle of the focal mechanism. In this study, we model the SH wave seismograms of this event in an attempt to further constrain the focal mechanism.

Methods

Theoretical S wave arrival times were computed given the ISC reported epicentral location and origin time. The microfiche chips were examined and an attempt was made to locate the S arrivals. On many records the arrivals were too small to accurately identify. A set of 16 records was determined to have clear enough arrivals to digitize.

Both the north-south and east-west components of the long-period WWSSN records were digitized. The digitized records were then resampled to produce time series with identical start times and time increments. These components were then rotated (projected) to produce a radial component, along the direction of wave propagation, and a transverse component, perpendicular to the direction of wave propagation. The direction of wave propagation is computed using spherical geometry and the location of the source and receiver. The SH waves should be present only on the transverse component. The transverse components were then modeled with synthetic seismograms, and the focal mechanism parameters altered to achieve the best fit at all stations.

Results

The depth and crustal model used by Andrews (previous abstract) were used as initial starting points for the SH modeling. These parameters were observed to provide the best fits for the SH waves as well. In particular, the S waves should show as much if not more effect of the crustal low velocity zone as the P waves since both S wave velocity and attenuation are more sensitive to partial melting than the P velocity and attenuation. Synthetics were created with and without the low velocity zone. Some improvements in the fits at stations to the east were observed using the crustal model with the low velocity zone. The SH waves were best fit with a depth of 4.0 km.

The strike, dip and slip angle determined by Andrews produced acceptable fits at most stations indicating that the general mechanism was correct. However, the fits at stations to the east of the epicenter such as BEC and MAL required a change in the mechanism. The strike was rotated more nearly north, the dip was decreased slightly, and the slip angle was decreased to move these stations closer to the SH nodal lines. The best fit mechanism, based on the SH wave modeling is shown in Figure 1. The strike is N5°W, the dip is 55°E, and the slip angle is 250°. The mechanism obtained by Andrews is also plotted in Figure 1. Figure 2 shows a set of best fit synthetic and observed SH seismograms. The SH focal sphere, shown in Figure 2, exhibits SH nodal **lines** rather than P nodal **planes**. The SH nodal lines are complex geometric figures that show the directions where no horizontally polarized S waves are radiated. P wave synthetics were calculated using the revised focal mechanism parameters and were observed to be nearly iden-